doi:10.1016/j.jmb.2009.11.063 J. Mol. Biol. (2010) 396, 501–509

JMB

Available online at www.sciencedirect.com

ScienceDirect

ELSEVIER

Myosin Isoform Determines the Conformational Dynamics and Cooperativity of Actin Filaments in the Strongly Bound Actomyosin Complex

Ewa Prochniewicz[1], Harvey F. Chin[2], Arnon Henn[2], Diane E. Hannemann[2], Adrian O. Olivares[2], David D. Thomas[1]* and Enrique M. De La Cruz[2]*

[1]*Department of Biochemistry, Molecular Biology, and Biophysics, University of Minnesota, Minneapolis, MN 55455, USA*

[2]*Department of Molecular Biophysics and Biochemistry, Yale University, New Haven, CT 06520, USA*

Received 29 July 2009; received in revised form 6 October 2009; accepted 27 November 2009
Available online 4 December 2009

We used transient phosphorescence anisotropy to detect the microsecond rotational dynamics of erythrosin-iodoacetamide-labeled actin strongly bound to single-headed fragments of muscle myosin subfragment 1 (S1) and non-muscle myosin V (MV). The conformational dynamics of actin filaments in solution are markedly influenced by the isoform of bound myosin. Both myosins increase the final anisotropy of actin at substoichiometric binding densities, indicating long-range, non-nearest neighbor cooperative restriction of filament rotational dynamics amplitude, but the cooperative unit is larger with MV than with muscle S1. Both myosin isoforms also cooperatively affect the actin filament rotational correlation time, but with opposite effects: muscle S1 decreases rates of intrafilament torsional motion, while binding of MV increases the rates of motion. The cooperative effects on the rates of intrafilament motions correlate with the kinetics of myosin binding to actin filaments such that MV binds more rapidly and muscle myosin binds more slowly to partially decorated filaments than to bare filaments. The two isoforms also differ in their effects on the phosphorescence lifetime of the actin-bound erythrosin iodoacetamide: while muscle S1 increases the lifetime, suggesting decreased aqueous exposure of the probe, MV does not induce a significant change. We conclude that the dynamics and structure of actin in the strongly bound actomyosin complex are determined by the isoform of the bound myosin in a manner likely to accommodate the diverse functional roles of actomyosin in muscle and non-muscle cells.

Edited by R. Craig

Keywords: actin; dynamics; phosphorescence; non-muscle myosin; allostery

Introduction

Elucidation of the structure of the actomyosin complex is critical for understanding the mechanism of contractility. Crystallographic and electron microscopy studies performed on isolated muscle and non-muscle myosin isoforms have detected structural changes in myosin light chain domains and actin-binding regions in response to binding of nucleotides and nucleotide analogs, indicating that all myosins undergo structural transitions during the force-generating actomyosin ATPase cycle.[1–7] Structures of strongly bound actomyosin complexes, obtained by fitting crystal structures of muscle actin and the myosin head into a three-dimensional reconstruction from electron micrographs of the complex, showed remarkable similarities at the

**Corresponding authors.* D. D. Thomas is to be contacted at Department of Biochemistry, Molecular Biology, and Biophysics, University of Minnesota, Minneapolis, MN 55455, USA; E. M. De La Cruz, Department of Molecular Biophysics and Biochemistry, Yale University, New Haven, CT 06520, USA. E-mail addresses: ddt@ddt.biochem.umn.edu; enrique.delacruz@yale.edu.

Present address: A. O. Olivares, Department of Biology, Massachusetts Institute of Technology, Cambridge, MA 02139, USA.

Abbreviations used: S1, subfragment 1; MV, myosin V; TPA, transient phosphorescence anisotropy; ErIA, erythrosin iodoacetamide.

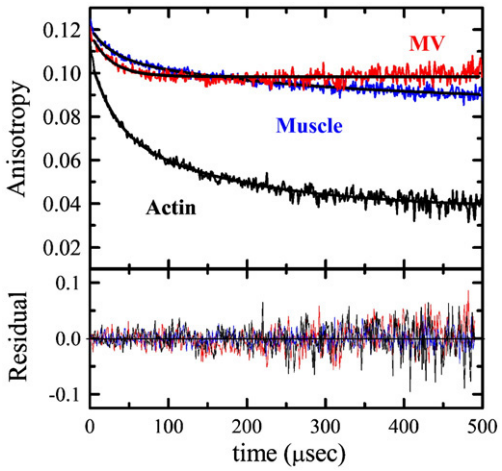

Fig. 1. The effects of muscle S1 and MV on TPA decays of actin in the absence of nucleotide. S1/A = 1.2, KMg50, 0.5 U/ml of apyrase. Smooth lines represent fits to the sum of two exponential terms (Eq. (2)).

interface between actin and various myosin isoforms, such as skeletal and smooth muscle subfragment 1 (S1),[6,8] myosin V (MV),[5] and myosin VI,[9] supporting a common structural basis for the mechanism of actomyosin function.

On the other hand, biochemical studies showed that the extent of actin-activated ATPase, as well as the *in vitro* sliding speed of actin filaments, strongly depends on the interacting myosin isoform.[10–13] Kinetic studies indicate that these biochemical differences probably reflect differences in the rate-limiting step of the actomyosin ATPase for different myosin isoforms. For example, the rate-limiting step for acto-MV ATPase is ADP release,[14,15] while the rate-limiting step for acto-muscle S1 ATPase is a combination of ATP hydrolysis and phosphate (P_i) release.[16] Consequently, MV spends most of its actomyosin ATPase cycle strongly bound to actin,[14] which contributes to processive motility, while non-processive muscle S1 spends most of the ATPase cycle in the low-affinity, weakly bound state and enters a strongly bound state after ATP hydrolysis and P_i release. Thus, the molecular mechanism of interaction between actin and various myosin isoforms is fine-tuned to the isoform-specific functions and properties of myosin. The goal of our study was to determine whether the mechanism of this interaction involves isoform-specific changes in the structural dynamics of actin filaments.

We used transient phosphorescence anisotropy (TPA) to determine the dynamics of actin in complex with the strongly bound, nucleotide-free state of muscle S1 or a truncated, single-headed non-muscle MV construct. Our previous studies established that the dynamics of actin on the microsecond time scale, as detected by TPA, is significantly affected by a variety of actin-binding proteins, such as skeletal muscle myosin, gelsolin, cofilin, and dystrophin.[17–22] The dynamics and cooperative interactions depend on the bound protein, indicating that actin dynamics are determined by protein-specific interactions at the binding interface. Our results show that the conformational dynamics of actin filaments and therefore the binding interface also depend on the type of interacting myosin.

Results

The effects of muscle S1 and MV on TPA of actin

Time courses of TPA decays (Fig. 1) measured in KMg50 buffer and the absence of nucleotide show that binding of saturating amounts of muscle S1 and MV to erythrosin iodoacetamide (ErIA)-actin results in a substantial increase in the final anisotropy, indicating that both myosins decrease the amplitude of actin's rotational microsecond dynamics. The effects of the two myosin isoforms on actin dynamics were analyzed in more detail by performing measurements over a wide range of myosin concentrations (from 0.025 to 0.6 μM). Under these conditions, myosin binds actin (0.5 μM) stoichiometrically to saturation since the K_d is in the range of 0.004–0.03 μM for nucleotide-free muscle S1 and MV.[18,23] The interaction of these myosins with actin filaments is not significantly affected by ErIA labeling of actin[18] (Supplementary Material).

Changes in actin dynamics resulting from an increased fraction of bound muscle S1 and MV were first analyzed according to the effects on the final anisotropy (Fig. 2), defined as the average anisotropy over a 400- to 500 -μs time window, which is the most sensitive and direct indicator of changes in the amplitude of actin's microsecond rotational dynamics.[19] Fitting the changes in the final anisotropy to a one-dimensional linear lattice model (Eq. (1)) shows that changes induced by the two myosins display long-range, non-nearest neighbor cooperativity. However, the extent of cooperativity, defined as the number of filament subunits (cooperative unit, N) affected by a single bound myosin, is much higher for MV ($N = 12.61 \pm 0.74$) than for muscle S1 ($N = 4.33 \pm 0.56$).

Experiments performed in the presence of ADP and in the absence of Mg^{2+} or in the presence of MgADP did not detect significant effects of the

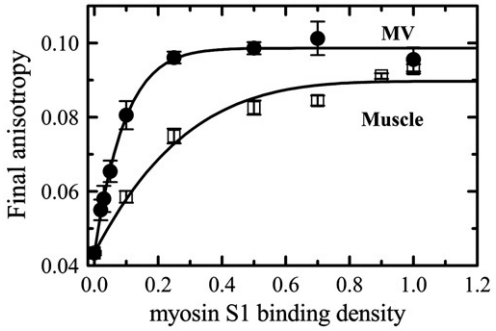

Fig. 2. The effects of increasing fractions of strongly bound muscle S1 and MV on the final anisotropy of actin.

nucleotide on anisotropy decays of actin in the same range of bound MV concentrations (data not shown). This observation indicates that TPA does not distinguish between the documented effects of ADP- and nucleotide-free MV.[23,24]

The effects of muscle S1 and MV on actin are further compared using model-independent analysis of TPA decays (Eqs. (2) and (3)), which yielded two more parameters of actin dynamics: the initial anisotropy and the average rotational correlation times. The initial anisotropy reflects amplitudes of sub-microsecond motions (immobilized erythrosin phosphorescent probe has an initial anisotropy of 0.205). The binding of either myosin increases the initial anisotropy of actin, indicating decreased amplitudes of these motions, and in this case, both isoforms have similar effects (data not shown). Both myosin isoforms also affect the average correlation time $\langle\phi\rangle$, indicating changes in the rates of intrafilament rotational motions (Fig. 3), but the changes are in the opposite directions. While binding of MV decreases the value of $\langle\phi\rangle$, binding of muscle S1 increases it. These data indicate that binding of MV significantly increases the rates of intrafilament motions, while binding of muscle S1 decreases them. In both cases, changes in $\langle\phi\rangle$ are cooperative, but the fit to the linear lattice model showed that the extent of cooperative unit (N) depends on the myosin isoform. As observed for the final anisotropy (Fig. 2), MV is more cooperative ($N=5.94\pm2.13$) than muscle S1 ($N=1.95\pm0.52$). These values of N are different from those obtained by analysis of the final anisotropy (Fig. 2), indicating uncoupling between molecular changes associated with amplitudes and rates of intrafilament motions.

The effects of muscle S1 and MV on the phosphorescence intensity of actin

The analyses of phosphorescence intensity decays of actin in the presence of increasing fractions of bound muscle S1 and MV show that these myosins have substantially different effects on the average phosphorescence lifetime $\langle\tau\rangle$ of actin (Fig. 4). Binding of MV induces small—up to 13%—and non-cooperative changes in the $\langle\tau\rangle$ of actin (Fig. 4),

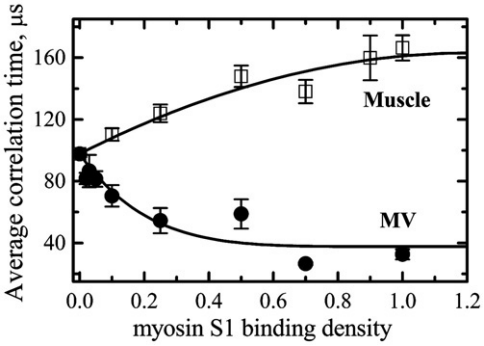

Fig. 3. The effects of increasing fractions of strongly bound muscle S1 and MV on the average correlation time $\langle\phi\rangle$ of actin.

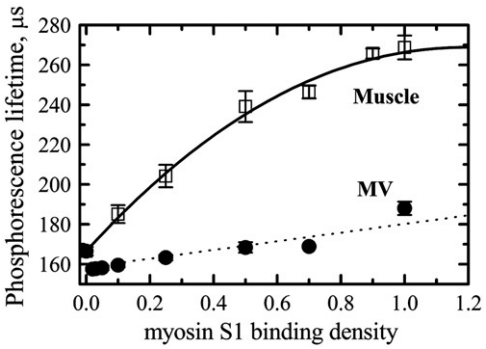

Fig. 4. The effects of strongly bound muscle S1 and MV on the average phosphorescence lifetime of actin-conjugated ErIA. The $\langle\tau\rangle$ in the presence of muscle S1 is fitted to the linear lattice model (Eq. (1)), and the $\langle\tau\rangle$ in the presence of MV is represented by the linear fit for visualization.

while muscle S1 increases $\langle\tau\rangle$ by about 61%, and the increase is cooperative, with an N of 2.06 ± 0.17. Since $\langle\tau\rangle$ is very sensitive to the quenching action of oxygen in solution, detected differences indicate that each myosin induces different, isoform-specific local structural changes in the environment of the probe conjugated to the C-terminus of actin.

The effect of myosin binding to actin on binding rate

The TPA results indicate that MV binding to actin filaments induces structural changes in the actin in a cooperative manner, affecting between ~6 and 13 (Figs. 2 and 3) actin subunits, while muscle S1 shows less cooperative changes in the actin filament. The functional effect of these structural changes on the actin filament was evaluated by measuring the rate of myosin binding to pyrene actin filaments partially decorated with varying amounts of either MV or muscle S1. The observed rate constant of binding for MV to pyrene actin increases as a function of the prebound MV binding density, from 62 s^{-1} for bare filaments ($k_+=62$ μM^{-1} s^{-1}) to a maximal value of ~66 s^{-1} when filaments are decorated at ~10% with prebound MV ($k_+=66$ μM^{-1} s^{-1}) (Fig. 5). The relative increase in the rate constant is small (~5%–10%) but statistically significant (ANOVA, $p<0.02$). Fitting the data to the linear lattice model indicates that the accelerated binding has a cooperativity of $N=15.1\pm5.2$ subunits, in close agreement with the cooperative unit associated with intrafilament motions (Fig. 3), suggesting that the acceleration of binding for subsequent MV molecules occurs because vacant filament sites have adopted the more dynamic MV-bound conformation.

In the presence of ADP, the effect of prebound MV on the observed binding rate constant is more pronounced than that in the absence of nucleotide (Fig. 5), suggesting that filament dynamics are greater although they were not detected by TPA, perhaps because they occur on a slower time scale. The increase in the mole fraction of the prebound MV

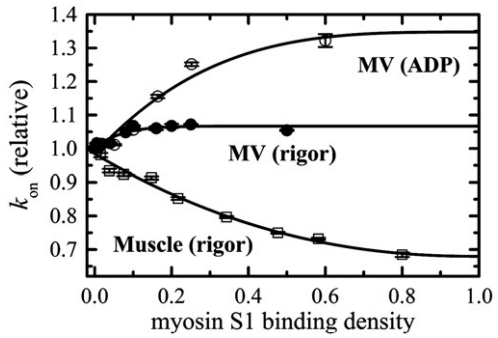

Fig. 5. The effects of the prebound S1 binding density on the relative k_{on} of myosin binding to pyrene actin for muscle S1 (squares), MV in the absence of nucleotide (filled circles), and MV in the presence of 20 μM MgADP (empty circles). Data points represent fits to averages of two to four individual time courses at the indicated prebound S1 density. The concentration dependence is fitted to the linear lattice model (Eq. (1)). Uncertainties represent errors in the fit.

increased the rate constant by a statistically significant 30% (ANOVA, $p<0.001$), from ~40 to ~50 s^{-1} under our experimental conditions, with $N=3.4\pm1.0$.

In contrast, muscle S1 displays negative cooperativity in binding actin filaments, as reported previously.[25] The observed rate constant for muscle S1 binding to pyrene actin decreases as a function of the prebound muscle S1 binding density (Fig. 5), and the maximum effect observed at a prebound density of >80% is an ~30% decrease in the observed rate constant for binding. Prebound muscle S1 shows less cooperativity than MV in effect on binding rate to pyrene actin with $N=2.2\pm0.3$, in agreement with the TPA results. The observation of opposing effects on binding rate constants based on the myosin isoform prebound to actin in experiments performed in parallel eliminates the possibility that the observed effects are due to experimental artifacts and indicates that the conformational dynamics of intrafilament motions is linked to myosin binding.

Acceleration of the observed MV binding rate constant can arise from an increase in the association rate constant, the dissociation rate constant, or both. We favor an interpretation in which the more rapid observed rate constant results from a more rapid association rate constant of MV since an increase in the dissociation rate constant by several orders of magnitude is required to account for the magnitude of change observed. Thus, both MV-induced and muscle S1-induced changes in actin dynamics and structure are associated with isoform-specific effects on the rate of myosin binding to vacant sites on the filament.

Comparison of the proposed regions of strong interaction of muscle S1 and MV isoforms with actin

Structure alignment of muscle S1 (Protein Data Bank code 2MYS) and MV (Protein Data Bank code 1OE9) showed 36.3% sequence homology between the two myosins, indicating substantial differences in their primary structures. We focused specifically on differences within the sequences of the proposed regions of interaction with actin: loop 2, lower 50K domain, "cardiomyopathy loop," and the secondary binding site for the neighboring actin monomer[8] (Fig. 6). The most prominent difference was found in the length of loop 2, which is much longer in MV (52 residues) than in muscle S1 (35 residues). Furthermore, all three regions of the primary actin binding site (loop 2, lower 50K domain, and the cardiomyopathy loop) show myosin-dependent differences in overall charge and amino acid composition. The secondary actin binding site shows difference in amino acid composition, while its length (25 residues in MV and 29 residues in muscle S1) and charge (+4 in MV and +4.2 in muscle S1) are similar. Thus, cumulative effects of differences in the regions of interaction with actin could provide major contribution to the differences in the effects of these two myosins on actin dynamics and their binding kinetics.

Discussion

Actin rotational dynamics in the strongly bound complex

The principal finding of this study is that the dynamics and structure of actin in the actomyosin complex substantially depend on the kind of bound myosin isoform—muscle S1 or non-muscle MV. Cooperative increase in the final anisotropy of actin with an increasing fraction of bound myosin (Fig. 2)

```
Loop2
 MV   F594-L645  FQDEEKAISPTSATPSGRVPLSRT
 MS1  F624-L658  FATYGGEAEGGGGKKGGKKKGSSF
 MV              PVKPAKARPGQTSKEHKKTVGHQFRNSL  (+6.2)
 MS1             ----------------QTVSALFRENL  (+3.0)
Lower 50K domain
 MV   L499-L533  LIEAKMGVLDLLDEECKMPKGSDDTWAQKLYNTHL (-2.9)
 MS1  L524-L560  LIEXPMGIFSILEEECMFPKATDTSFXNXLYDEHL (-5.9)
Cardiomyopathy loop
 MV   M372-I392  MAHWL--CHRKLATATETYIKPI (+2.1)
 MS1  L399-G417  LLKALCYPRVGVGN---EAVTXG (+1.0)
Secondary actin binding site
 MV   N534-V357  N-KCALFEKPRL---SNKAFIIKHFADKV (+4.0)
 MS1  G561-V589  GKSNNFQKPKPAKGKAEAHFSLVHYAGTV (+4.2)
```

Fig. 6. Structural alignment of the proposed regions of interaction of muscle S1 (MS1) and MV with actin. Numbers in parentheses show charges of the peptides calculated using Innovagen's Peptide Property Calculator program.

shows that while each myosin restricts amplitudes of motions of several protomers in an actin filament, bound MV allosterically affects a significantly longer segment of the filament than muscle S1. Each myosin also affects rates of intrafilament motions as indicated by changes in the rotational correlation time, but while MV increases the rates, muscle myosin has the opposite effect, decreasing the rates (Fig. 3). It is also noticeable that the extent of cooperativity for $\langle\phi\rangle$ is different from that for final anisotropy (Fig. 2), indicating isoform-specific uncoupling between molecular changes associated with amplitudes and rates of intrafilament motions. That is, the increased rates of motion do not simply arise from higher amplitude fluctuations. Rather, they suggest isoform-specific changes in the intrafilament flexibility of actin.[22] This interpretation suggests that actin is more flexible in complex with MV than with muscle S1. This increased torsional flexibility likely contributes to the more rapid MV binding kinetics (Fig. 5).

The isoform-dependent effects on actin dynamics cannot be due to differential effects of actin-bound ErIA or phalloidin on interaction with each myosin. Our previous study found that ErIA label does not affect strong binding affinity of muscle S1[18] and that phalloidin, while necessary to stabilize labeled actin from depolymerization and denaturation,[26] does not affect functional interaction with myosin.[19,27] Furthermore, phalloidin-stabilized actin has been used in experiments demonstrating significant differences in the kinetics of acto-muscle S1 and acto-MV,[14] as well as in the processivity of MV and muscle myosin in *in vitro* motility assay.[28–30]

While our study was performed using skeletal muscle actin, we cannot exclude the possibility that isoform-specific effects of myosins on actin dynamics will be different for non-muscle actin, which is the natural partner of MV but not of muscle myosin. However, this possibility does not affect the validity of our approach: our results provide structural complement to previously detected differences in the function and kinetics of acto-MV and acto-muscle myosin, which were detected using skeletal muscle actin (e.g., Ref. 14). In addition, the effects of actin isoform on MV enzymology are minimal.[31]

The observed reduction in correlation time and increased final anisotropy of actin with MV qualitatively resemble changes previously detected upon binding of the actin-binding proteins dystrophin and utrophin, which were proposed to result in an increased resistance of filaments to breaking by the contractile force of muscle.[22] By analogy, decreased correlation time and increased final anisotropy of actin upon binding of MV could be involved in the mechanism of stabilizing intracellular actin during processive transport, which is much more dynamic in non-muscle cells than in the well-organized contractile apparatus of skeletal muscle.

Different effects of MV and muscle myosin could also represent a molecular adaptation of MV for transport along a filament, where a recessively moving myosin has to accommodate 36 -nm steps, corresponding to actin's pseudo-helical repeat of myosin-binding regions. The number of protomers cooperatively affected by one head (Fig. 2) is comparable with 11–15 protomers separating two heads of actin-bound MV,[32] suggesting that conformational changes in actin induced by one bound head could be transferred along the filament and affect the binding site for another head. This possibility is supported by the results of kinetic experiments (Fig. 5). The rate of MV binding is accelerated by the presence of the prebound MV, suggesting that myosin-induced changes in actin structure and dynamics provide a functional adaptation, affecting binding of MV to the next site during processive motility. Regulated binding of other myosin isoforms via myosin-induced structural changes in an actin filament is supported by electron microscopy and optical trap studies.[33,34]

Myosin-induced local changes in actin

Isoform-specific effects of myosin on the structure of actin protomers were observed in electron microscopy studies, in which three-dimensional reconstructions of the complexes of smooth and skeletal muscle myosins with actin revealed myosin-specific structural changes in subdomain 1 and in the structurally coupled subdomain 2.[6] Our current analysis of the lifetime of the actin-bound ErIA probe indicates that at least the C-terminus in subdomain 1 is differently affected by muscle S1 than by MV. A cooperative increase in the ErIA lifetime upon binding of muscle S1 indicates changes in the environment of the probe resulting in increased protection from the quenching effect of oxygen; however, the effect of MV on ErIA lifetime is much less pronounced, indicating significantly smaller structural changes (Fig. 4). Thus, MV presumably affects the environment of Cys374, but in a different manner relative to muscle S1. Since the changes in the state of the C-terminus of actin are associated with changes in the intermonomer contacts and structure of actin filament,[35] possible different effects of the two myosin isoforms on this region can provide one of the explanations for the different effects on the dynamics of bound actin. It is possible that the myosin-linked dissociation of stabilizing actin-filament-associated ions contributes to the enhanced filament dynamics, as reported for cofilin.[36]

Structural transitions in myosin during binding to actin

The alignment of crystal structures of muscle S1 and MV showed that despite overall similarity of the structures, the structures are not identical and isoform-specific differences between nucleotide-free myosins in solution exist, particularly in the extent of actin-binding cleft closure.[3] The state of the actin-binding cleft in free myosin may be crucial to the mechanism of interaction with actin since it has been predicted that the cleft has to close to create the rigor complex with actin,[8,37] presumably by

movement of subdomains in the myosin head.[3,6] This prediction is supported by three-dimensional reconstruction of cryo-electron micrographs of actomyosins, where actin-bound muscle S1 and MV show a closed actin-binding cleft.[5,6]

Isoform-specific conformational changes in muscle S1 and MV associated with actin binding are further supported by kinetic studies: while temperature-dependent binding of muscle S1 indicates different structural states before and after binding to actin,[38] lack of temperature dependence for nucleotide-free MV binding to actin indicated that binding is limited by encounter (i.e., conformational changes after encounter are more rapid) and/or the structural state of the MV catalytic domain in solution is nearly equivalent to that after binding to actin.[14]

We propose that isoform-specific effects on actin dynamics and structure (Figs. 2–4) are associated with isoform-specific structural transitions in myosins during binding to actin. The proposed coupling of structural transitions in myosin with actin dynamics is supported by our previous TPA studies. We have detected coupling between the order–disorder transition in muscle S1 and the transition in the dynamics of the interacting actin during the strong-to-weak transition in the actomyosin ATPase cycle.[19] Furthermore, perturbation of myosin structure by oxidative modifications affects the extent of strong-to-weak transition in actin, indicating that the dynamics of actin interacting with myosin depends on the structural state of myosin.[27]

Structural differences between muscle S1 and MV

Heavy chains

Isoform-specific structural transitions in myosin during binding to actin are probably associated with an overall low (36.3%) sequence homology between the heavy chains of the two isoforms, particularly with differences in the amino acid sequences in the proposed actin-binding regions of muscle S1 and MV (Fig. 6). The most prominent differences are in loop 2, which is disordered in unbound myosin but becomes ordered in the strongly bound complex.[5,6] The length of the loop and structural changes accompanying binding to actin are proposed to be essential for the mechanism of processive movement of MV, which is not observed for muscle S1.[5] It has been suggested that the net positive charge of this loop, which is about twice that of muscle S1, allows MV to bind actin with high affinity, preventing its diffusion from actin and increasing processivity.[5] The crucial role of the structure of loop 2 in the interaction with actin is further supported by mutational studies of *Dictyostelium* myosin, which have shown that charge, length, and amino acid sequence affect myosin's affinity to actin.[11] Mutational studies on *Dictyostelium* myosin also found that formation of the actomyosin complex is substantially affected by site-specific mutations in other regions of the primary binding site—lower 50K domain and cardiomyopathy loop.[39,40] This suggests that differences in these regions of muscle S1 and MV (Fig. 6) provide further contributions to the different structural effects of the two myosin isoforms on actin.

Light chains

The myosin isoforms used in this study have differences not only in the sequences of heavy chains but also in the type of the essential light chains: muscle S1 has two isoforms of the essential light chains, while MV has been coexpressed with one human essential light chain.[14,31] A possible role of the type of light chain in the structure of the actomyosin complex is suggested by their pronounced functional effects, as observed for muscle myosin. Biochemical and physiological studies showed that light chain isoforms affect calcium regulation of fiber shortening,[41] the extent of actin-activated ATPase, and the speed of actin filament sliding in *in vitro* motility assay.[42–44] Electron microscopy showed that the A1 essential chain of muscle S1 interacts with the C-terminus of actin[45] in the absence and in the presence of ATP.[46] In the case of MV, the kind of light chain isoform was shown to affect kinetic properties of MV;[31] however, its role in the structure of the actomyosin complex has not been determined.

Summary of results

We report that non-muscle MV, similar to muscle S1, restricts the microsecond dynamics of strongly bound actin. However, specific parameters of actin dynamics, including final anisotropy, rates of intra-filament motions, and the environment of the actin C-terminus, are dependent on the kind of bound myosin isoform. Partial saturation of filament with MV allosterically affects vacant filament subunits, putting them in a "myosin-bound" conformation. These non-nearest neighbor effects on filament dynamics increase the association of subsequent MV molecules since incoming myosin molecules can bind actin without having to introduce this change. It has been proposed that actin filaments assume multiple conformations[47] and that structural changes induced by various binding proteins, including different myosin isoforms, likely reflect a shift in this conformational equilibrium toward one most suitable for interaction. We propose that such conformational flexibility of actin allows adjustment of the structure of its binding interface to the structure and function of specific myosin isoforms for optimal performance of the actomyosin complex in a variety of intracellular structures.

Materials and Methods

Protein preparations

Skeletal muscle actin was prepared from rabbit skeletal muscle as previously described,[19] by extracting acetone

powder in cold water, polymerizing with 30 mM KCl for 1 h at room temperature, and centrifuging for 30 min at 350,000*g*. The pellet was suspended in G-Ca buffer (5 mM Tris, pH 7.5, 0.5 mM ATP, 0.2 mM $CaCl_2$); pH values of all buffers are reported for 25 °C.

Muscle S1 was obtained by α-chymotryptic digestion of rabbit skeletal muscle myosin, as described previously.[19]

The cDNA for chicken MV was truncated at the Arg792 codon, generating a construct consisting of the motor domain and the first IQ motif. The human essential light chain (LC-1sa) was subcloned into pVL1393 for baculovirus expression and coexpressed with MV-1IQ. Expression and purification of MV were performed as described previously.[14]

Purified myosins were stored in 50 mM KCl, 0.2 mM $CaCl_2$, 10 mM imidazole, pH 7.0, 1 mM DTT, and 50% glycerol at −20 °C.

Labeling of actin at Cys374 with ErIA (AnaSpec) was performed as described previously.[19] Actin (48 μM) was polymerized with 50 mM KCl in 20 mM Tris, pH 7.5; ErIA freshly dissolved in DMF was added at a concentration of 480 μM, and the sample was incubated for 2 h at 25 °C. Labeling was stopped by adding 10 mM DTT; actin was ultracentrifuged for 30 min at 350,000*g*; pellets were suspended in G-Ca buffer, clarified by 10 min of centrifugation at 300,000*g*; and actin was polymerized for 30 min at 25 °C by adding 50 mM KCl or 2 mM $MgCl_2$. After ultracentrifugation for 30 min at 350,000*g*, pellets were suspended in K50 buffer (50 mM KCl, 10 mM imidazole, pH 7.0, 0.2 mM $CaCl_2$) or KMg50 buffer (50 mM KCl, 2 mM $MgCl_2$, 10 mM imidazole pH 7.0, 0.2 mM $CaCl_2$) containing 0.2 mM ATP, and the labeled F-actin was immediately stabilized against depolymerization and denaturation by adding 1 molar equivalent of phalloidin. The stabilization of actin by phalloidin was critical since multiple control experiments showed that phalloidin-free ErIA-actin filaments are unstable and show time-dependent depolymerization and/or denaturation at pH >7.0. The extent of labeling (mol dye/mol actin), determined by measuring absorbance of labeled actin at 538 nm and assuming a molar extinction coefficient of 83,000, was 0.83± 0.13 (mean±SD, $n=11$).

The concentrations of myosin S1 and labeled actin were measured by the Bradford protein assay[48] (BioRad) using bovine serum albumin and unlabeled actin of known concentration, respectively, as a standard.

TPA experiments

Phalloidin-stabilized ErIA-F-actin was diluted in KMg50 buffer to 0.5 μM, and acto-S1 complexes were formed by adding 0.025–0.6 μM S1, as indicated in the text. All samples prior to measurement were incubated for 20 min with 0.5 U/ml of apyrase to remove residual ATP from actin. Oxygen was removed from the sample by 5 min of incubation with glucose oxidase (55 μg/ml), catalase (36 μg/ml), and glucose (45 μg/ml) to prevent photobleaching of the dye during TPA measurement.[19]

Phosphorescence was measured at 25 °C as described previously[21] with slight modification of the TPA spectrometer. Actin-bound ErIA was excited with a vertically polarized 1.2-ns pulse from an FDSS 532-150 laser (CryLas) at 532 nm, operating at a repetition rate of 100 Hz. Phosphorescence emission was selected by a 670 -nm glass cutoff filter (Corion), detected by a photomultiplier (R928, Hamamatsu), and digitized by a transient digitizer (CompuScope 14100, GaGe) at a time resolution of 1 μs/channel. The time-resolved phosphorescence anisotropy decay was calculated as $r(t)=[I_v(t)-GI_h(t)]/[I_v(t)+2GI_h(t)]$, where $I_v(t)$ and $I_h(t)$ are vertically and horizontally polarized components of the emission signal, respectively, detected at 90° with a single detector and a Polaroid sheet polarizer that alternated between the two orientations every 500 laser pulses. G is an instrumental correction factor that is determined by performing the measurement with horizontally polarized excitation, for which the corrected anisotropy value is set to zero. The time-dependent anisotropy decays of free actin and its complexes with muscle S1 were obtained by recording 30 cycles of 1000 pulses (500 in each orientation of the polarizer).

TPA data analysis

Final anisotropy was defined as the average value of r in the time window from 400 to 500 μs, which has been shown previously to provide the most sensitive and precise measurement of actin's microsecond rotational dynamics.[17] The effects of strongly bound S1 on the final anisotropy of actin were analyzed in terms of the linear lattice model as in our previous work,[17,18] assuming that perturbation of one protomer in an actin filament affects a segment containing N protomers:

$$r = r_{max} - (r_{max} - r_{actin})(1-x)^N \quad (1)$$

where r_{actin} and r_{max} are the limiting values of anisotropy at 0 and infinite concentrations of S1, respectively, and $x=$ [S1]/[actin] binding density. The adjustable parameters in the least-squares fit were r_{max} and N.

Other parameters of TPA decay (initial anisotropy r_0 and correlation times ϕ_1 and ϕ_2) were determined by fitting the decay to the double exponential and a constant r_∞:

$$r(t) = r_1\exp(-t/\phi_1) + r_2\exp(-t/\phi_2) + r_\infty \quad (2)$$

This method of analysis was established previously[17,18,49] and was validated by comparing residuals and χ^2 for fits: fits of the current data were optimal for $n=2$ with residuals not exceeding 2% of the maximum anisotropy. For model-independent comparison of the effects of the myosin isoforms used, the component lifetimes and amplitudes of the decay were used to calculate a single average correlation time $\langle\phi\rangle$:

$$\langle\phi\rangle = (\phi_2 r_1 + \phi_2 r_2)/(r_1 + r_2) \quad (3)$$

The phosphorescence intensity decays of actin-bound ErIA $I(t)=(I_v(t)+2*GI_h(t))/3$ were best fitted to three exponential terms:

$$I(t) = a_1\exp(-t/\tau_1) + a_2\exp(-t/\tau_2) + a_3\exp(-t/\tau_3) \quad (4)$$

The a_i amplitudes and the τ_i triplet excited lifetimes were used to calculate a single average lifetime $\langle\tau\rangle$:

$$\langle\tau\rangle = (a_1\tau_1 + a_2\tau_2 + a_3\tau_3)/(a_1 + a_2 + a_3) \quad (5)$$

Transient kinetic fluorescence measurements

Transient kinetic measurements of MV binding to pyrene actin filaments were performed in KMg50 buffer [50 mM KCl, 2 mM $MgCl_2$, 1 mM ethylene glycol bis(β-aminoethyl ether)*N*,*N*′-tetraacetic acid, 1 mM DTT, 10 mM imidazole, pH 7.0] using an Applied Photophysics SX.18MV-R stopped-flow apparatus thermostated at 25± 0.1 °C. Actin was labeled with pyrene iodoacetamide as described previously.[14] Pyrene actin (100 nM) stabilized with an equimolar amount of phalloidin was preincubated with increasing concentrations of MV up to 1.2 mol MV/

mol actin in the presence of 0.1 U/ml of apyrase (no nucleotide) or 20 μM MgADP (+ADP). After 1 μM MV was added, the time course of fluorescence quenching of pyrene actin (λ_{ex} = 366 nm) was monitored at 90° through a 400-nm long-pass colored glass filter. Typically, two to four time courses were averaged and then fitted to a sum of exponential terms.[50] Errors are reported as standard errors of the fit. Data in Fig. 5 are fit to the linear lattice model presented in Eq. (1), with r_{actin} and r_{max} representing observed rate constants at 0 and infinite concentrations of S1, respectively.

Steady-state ATPase

The actin-activated steady-state ATPase of myosin was determined using the NADH-coupled assay.[14,15,50]

Statistical analysis of data

Each result is reported as mean±SEM, unless indicated otherwise. The statistical significance of differences was evaluated by one-way ANOVA, with Tukey post hoc tests performed for multiple comparisons. Differences were considered significant for $p < 0.05$.

Acknowledgements

This work was supported by grants from the National Institutes of Health to D.D.T. (AR32961, AG26160) and to E.M.D.L.C. (GM071688). E.M.D.L.C. is an American Heart Association Established Investigator (0940075N), a National Science Foundation Career Award recipient (MCB-0546353), and a Hellman Family Fellow. H.F.C. is supported by the National Institutes of Health through a predoctoral fellowship (F31 DC009143) and in part by grants from the American Heart Association (0655849T) and Yale Institute for Nanoscience and Quantum Engineering to E.M.D.L.C. We thank Octavian Cornea for assistance with preparation of the manuscript, Bengt Svensson for help with structural alignment of myosin isoforms, and Igor Negrashov for phosphorescence instrumentation and analysis software.

Supplementary Data

Supplementary data associated with this article can be found, in the online version, at doi:10.1016/j.jmb.2009.11.063

References

1. Himmel, D. M., Gourinath, S., Reshetnikova, L., Shen, Y., Szent-Gyorgyi, A. G. & Cohen, C. (2002). Crystallographic findings on the internally uncoupled and near-rigor states of myosin: further insights into the mechanics of the motor. *Proc. Natl Acad. Sci. USA*, **99**, 12645–12650.
2. Whittaker, M., Wilson-Kubalek, E. M., Smith, J. E., Faust, L., Milligan, R. A. & Sweeney, H. L. (1995). A 35-Å movement of smooth muscle myosin on ADP release. *Nature*, **378**, 748–751.
3. Coureux, P. D., Wells, A. L., Menetrey, J., Yengo, C. M., Morris, C. A., Sweeney, H. L. & Houdusse, A. (2003). A structural state of the myosin V motor without bound nucleotide. *Nature*, **425**, 419–423.
4. Houdusse, A. & Sweeney, H. L. (2001). Myosin motors: missing structures and hidden springs. *Curr. Opin. Struct. Biol.* **11**, 182–194.
5. Volkmann, N., Liu, H., Hazelwood, L., Krementsova, E. B., Lowey, S., Trybus, K. M. & Hanein, D. (2005). The structural basis of myosin V processive movement as revealed by electron cryomicroscopy. *Mol. Cell*, **19**, 595–605.
6. Volkmann, N., Ouyang, G., Trybus, K. M., DeRosier, D. J., Lowey, S. & Hanein, D. (2003). Myosin isoforms show unique conformations in the actin-bound state. *Proc. Natl Acad. Sci. USA*, **100**, 3227–3232.
7. Gulick, A. M., Bauer, C. B., Thoden, J. B. & Rayment, I. (1997). X-ray structures of the MgADP, MgATPgammaS, and MgAMPPNP complexes of the *Dictyostelium discoideum* myosin motor domain.. *Biochemistry*, **36**, 11619–11628.
8. Rayment, I., Holden, H. M., Whittaker, M., Yohn, C. B., Lorenz, M., Holmes, K. C. & Milligan, R. A. (1993). Structure of the actin–myosin complex and its implications for muscle contraction. *Science*, **261**, 58–65.
9. Menetrey, J., Bahloul, A., Wells, A. L., Yengo, C. M., Morris, C. A., Sweeney, H. L. & Houdusse, A. (2005). The structure of the myosin VI motor reveals the mechanism of directionality reversal. *Nature*, **435**, 779–785.
10. Rosenfeld, S. S. & Taylor, E. W. (1984). The ATPase mechanism of skeletal and smooth muscle actosubfragment 1. *J. Biol. Chem.* **259**, 11908–11919.
11. Murphy, C. T. & Spudich, J. A. (1999). The sequence of the myosin 50–20K loop affects myosin's affinity for actin throughout the actin–myosin ATPase cycle and its maximum ATPase activity. *Biochemistry*, **38**, 3785–3792.
12. De La Cruz, E. M., Ostap, E. M. & Sweeney, H. L. (2001). Kinetic mechanism and regulation of myosin VI. *J. Biol. Chem.* **276**, 32373–32381.
13. Yengo, C. M., De la Cruz, E. M., Safer, D., Ostap, E. M. & Sweeney, H. L. (2002). Kinetic characterization of the weak binding states of myosin V. *Biochemistry*, **41**, 8508–8517.
14. De La Cruz, E. M., Wells, A. L., Rosenfeld, S. S., Ostap, E. M. & Sweeney, H. L. (1999). The kinetic mechanism of myosin V. *Proc. Natl Acad. Sci. USA*, **96**, 13726–13731.
15. De La Cruz, E. M., Sweeney, H. L. & Ostap, E. M. (2000). ADP inhibition of myosin V ATPase activity. *Biophys. J.* **79**, 1524–1529.
16. White, H. D., Belknap, B. & Webb, M. R. (1997). Kinetics of nucleoside triphosphate cleavage and phosphate release steps by associated rabbit skeletal actomyosin, measured using a novel fluorescent probe for phosphate. *Biochemistry*, **36**, 11828–11836.
17. Prochniewicz, E. & Thomas, D. D. (1997). Perturbations of functional interactions with myosin induce long-range allosteric and cooperative structural changes in actin. *Biochemistry*, **36**, 12845–12853.
18. Prochniewicz, E. & Thomas, D. D. (2001). Site-specific mutations in the myosin binding sites of actin affect structural transitions that control myosin binding. *Biochemistry*, **40**, 13933–13940.

19. Prochniewicz, E., Walseth, T. F. & Thomas, D. D. (2004). Structural dynamics of actin during active interaction with myosin: different effects of weakly and strongly bound myosin heads. *Biochemistry*, **43**, 10642–10652.
20. Prochniewicz, E., Janson, N., Thomas, D. D. & De la Cruz, E. M. (2005). Cofilin increases the torsional flexibility and dynamics of actin filaments. *J. Mol. Biol.* **353**, 990–1000.
21. Prochniewicz, E., Zhang, Q., Janmey, P. A. & Thomas, D. D. (1996). Cooperativity in F-actin: binding of gelsolin at the barbed end affects structure and dynamics of the whole filament. *J. Mol. Biol.* **260**, 756–766.
22. Prochniewicz, E., Henderson, D., Ervasti, J. M. & Thomas, D. D. (2009). Dystrophin and utrophin have distinct effects on the structural dynamics of actin. *Proc. Natl Acad. Sci. USA*, **106**, 7822–7827.
23. Hannemann, D. E., Cao, W., Olivares, A. O., Robblee, J. P. & De La Cruz, E. M. (2005). Magnesium, ADP, and actin binding linkage of myosin V: evidence for multiple myosin V-ADP and actomyosin V-ADP states.. *Biochemistry*, **44**, 8826–8840.
24. Robblee, J. P., Cao, W., Henn, A., Hannemann, D. E. & De La Cruz, E. M. (2005). Thermodynamics of nucleotide binding to actomyosin V and VI: a positive heat capacity change accompanies strong ADP binding. *Biochemistry*, **44**, 10238–10249.
25. Blanchoin, L., Didry, D., Carlier, M. F. & Pantaloni, D. (1996). Kinetics of association of myosin subfragment-1 to unlabeled and pyrenyl-labeled actin. *J. Biol. Chem.* **271**, 12380–12386.
26. Prochniewicz, E., Spakowicz, D. & Thomas, D. D. (2008). Changes in actin structural transitions associated with oxidative inhibition of muscle contraction. *Biochemistry*, **47**, 11811–11817.
27. Prochniewicz, E. & Yanagida, T. (1990). Inhibition of sliding movement of F-actin by crosslinking emphasizes the role of actin structure in the mechanism of motility. *J. Mol. Biol.* **216**, 761–772.
28. Sakamoto, T., Amitani, I., Yokota, E. & Ando, T. (2000). Direct observation of processive movement by individual myosin V molecules. *Biochem. Biophys. Res. Commun.* **272**, 586–590.
29. Finer, J. T., Simmons, R. M. & Spudich, J. A. (1994). Single myosin molecule mechanics: piconewton forces and nanometre steps. *Nature*, **368**, 113–119.
30. Yanagida, T., Nakase, M., Nishiyama, K. & Oosawa, F. (1984). Direct observation of motion of single F-actin filaments in the presence of myosin. *Nature*, **307**, 58–60.
31. De La Cruz, E. M., Wells, A. L., Sweeney, H. L. & Ostap, E. M. (2000). Actin and light chain isoform dependence of myosin V kinetics. *Biochemistry*, **39**, 14196–14202.
32. Walker, M. L., Burgess, S. A., Sellers, J. R., Wang, F., Hammer, J. A., III, Trinick, J. & Knight, P. J. (2000). Two-headed binding of a processive myosin to F-actin. *Nature*, **405**, 804–807.
33. Tokuraku, K., Kurogi, R., Toya, R. & Uyeda, T. Q. (2009). Novel mode of cooperative binding between myosin and Mg^{2+}-actin filaments in the presence of low concentrations of ATP. *J. Mol. Biol.* **386**, 149–162.
34. Nishikawa, S., Homma, K., Komori, Y., Iwaki, M., Wazawa, T., Hikikoshi Iwane, A. *et al.* (2002). Class VI myosin moves processively along actin filaments backward with large steps. *Biochem. Biophys. Res. Commun.* **290**, 311–317.
35. Orlova, A., Prochniewicz, E. & Egelman, E. H. (1995). Structural dynamics of F-actin: II. Cooperativity in structural transitions. *J. Mol. Biol.* **245**, 598–607.
36. Cao, W., Goodarzi, J. P. & De La Cruz, E. M. (2006). Energetics and kinetics of cooperative cofilin–actin filament interactions. *J. Mol. Biol.* **361**, 257–267.
37. Yengo, C. M., De La Cruz, E. M., Chrin, L. R., Gaffney, D. P., II & Berger, C. L. (2002). Actin-induced closure of the actin-binding cleft of smooth muscle myosin. *J. Biol. Chem.* **277**, 24114–24119.
38. Taylor, E. W. (1991). Kinetic studies on the association and dissociation of myosin subfragment 1 and actin. *J. Biol. Chem.* **266**, 294–302.
39. Sasaki, N., Ohkura, R. & Sutoh, K. (2002). *Dictyostelium* myosin II as a model to study the actin–myosin interactions during force generation. *J. Muscle Res. Cell Motil.* **23**, 697–702.
40. Volkmann, N., Lui, H., Hazelwood, L., Trybus, K. M., Lowey, S. & Hanein, D. (2007). The R403Q myosin mutation implicated in familial hypertrophic cardiomyopathy causes disorder at the actomyosin interface. *PLoS ONE*, **2**, e1123.
41. Sweeney, H. L., Kushmerick, M. J., Mabuchi, K., Sreter, F. A. & Gergely, J. (1988). Myosin alkali light chain and heavy chain variations correlate with altered shortening velocity of isolated skeletal muscle fibers. *J. Biol. Chem.* **263**, 9034–9039.
42. Wagner, P. D., Slater, C. S., Pope, B. & Weeds, A. G. (1979). Studies on the actin activation of myosin subfragment-1 isoenzymes and the role of myosin light chains. *Eur. J. Biochem.* **99**, 385–394.
43. Lowey, S., Waller, G. S. & Trybus, K. M. (1993). Function of skeletal muscle myosin heavy and light chain isoforms by an *in vitro* motility assay. *J. Biol. Chem.* **268**, 20414–20418.
44. Timson, D. J. (2003). Fine tuning the myosin motor: the role of the essential light chain in striated muscle myosin. *Biochimie*, **85**, 639–645.
45. Milligan, R. A., Whittaker, M. & Safer, D. (1990). Molecular structure of F-actin and location of surface binding sites. *Nature*, **348**, 217–221.
46. Trayer, H. R. & Trayer, I. P. (1988). Fluorescence resonance energy transfer within the complex formed by actin and myosin subfragment 1. Comparison between weakly and strongly attached states. *Biochemistry*, **27**, 5718–5727.
47. Galkin, V. E., Orlova, A., Lukoyanova, N., Wriggers, W. & Egelman, E. H. (2001). Actin depolymerizing factor stabilizes an existing state of F-actin and can change the tilt of F-actin subunits. *J. Cell Biol.* **153**, 75–86.
48. Bradford, M. M. (1976). A rapid and sensitive method for the quantitation of microgram quantities of protein utilizing the principle of protein-dye binding. *Anal. Biochem.* **72**, 248–254.
49. Prochniewicz, E. & Thomas, D. D. (1999). Differences in structural dynamics of muscle and yeast actin accompany differences in functional interactions with myosin. *Biochemistry*, **38**, 14860–14867.
50. De La Cruz, E. M. & Ostap, E. M. (2009). Kinetic and equilibrium analysis of the myosin ATPase. *Methods Enzymol.* **455**, 157–192.